

# A BAYESIAN MULTITAPER METHOD FOR NONSTATIONARY DATA WITH APPLICATION TO EEG ANALYSIS

*P. Das and B. Babadi*

Department of Electrical & Computer Engineering, University of Maryland, College Park, MD 20742  
{proloy and behtash}@umd.edu

**Abstract**—Nonparametric spectral analysis using overlapping sliding windows is among the most widely used techniques in analyzing nonstationary time series. Although sliding window analysis is convenient to implement, the resulting estimates are sensitive to the subjective choice of window length and overlap extent and additionally lack precise statistical interpretation. In this paper, we propose a spectral estimator by explicitly modeling the spectral dynamics through combining the multitaper method with state-space models in a Bayesian estimation framework. The states are efficiently estimated using an instance of the Expectation-Maximization algorithm, from which the spectral estimates and their confidence intervals are constructed. We apply our proposed algorithm to synthetic data as well as real data from human EEG recordings, revealing significant improvements in spectral resolution and noise rejection.

## I. INTRODUCTION

Spectral analysis is regarded as one of the most essential tools in engineering and sciences, and has been long-established for extracting spectrotemporal information from time series data recorded from naturally occurring processes such as speech [1], electroencephalography (EEG) [2], oceanography [3], and seismic data [4]. In many of these applications, the exploratory nature of the analysis favors nonparametric techniques based on Fourier methods and Wavelets. In particular, the multitaper (MT) method for spectral analysis excels among the available nonparametric techniques due to its simplicity and control over bias-variance trade-off [5], [6].

While most nonparametric techniques are devised assuming second order stationarity of the time series, in many applications of interest, the energy of the various oscillatory components in the data exhibits dynamic behavior. In such cases, to get a meaningful spectrotemporal description, it is commonly assumed that the underlying process is quasi-stationary, i.e., the spectrum changes slowly over time. Thereby, the so-called spectrogram analysis is obtained by using sliding windows with overlap in order to capture nonstationarity [7], [8].

Although sliding window processing is widely accepted, it has several major drawbacks. First, window length and extent of overlap are subjective choices and can drastically change the overall attribute of the spectrogram if chosen poorly. Second, given that the estimate at each window is obtained by only the data within, it fails to fully capture the degree of smoothness inherent in the signal due to the common dynamic trends shared across multiple windows. Instead, the amount of overlap between adjacent windows

dictates the temporal smoothness of the estimates. Finally, the high statistical dependence of the estimates across windows induced by the underlying overlap, necessitates corrections for statistical assessment [9], thereby limiting the resulting test powers when multiple windows are involved.

Even though some of these shortcomings have been addressed by recent alternative approaches to nonstationary spectral analysis such as the Empirical Mode Decomposition (EMD) [10], synchrosqueezed wavelet transform [11], time-frequency reassignment [12], these methods assume that the underlying spectrotemporal components pertain to certain structures such as amplitude-modulated narrowband mixtures [10], [11] or chirp-like dynamics [12] etc. In addition to that, their implementations are computationally intensive.

In this paper, we address the foregoing challenges by integrating multitaper analysis with state-space modeling. State-space models provide a flexible and natural framework for analyzing systems which evolve with time [13], [14] and have been previously used for parametric [15], [16] and non-parametric [17] spectral estimation. The novelty of our approach is to develop a multitaper estimator capable of optimally combining data across windows and providing statistical confidence intervals. To this end, we construct a state-space model in which the underlying states pertain to spectral eigen-coefficients of the MT setting. We employ state dynamics that captures the spectrotemporal evolution of the signal, coupled with an observation model that captures the effect of additive measurement noise. We then employ Expectation-Maximization (EM) to find the maximum *a posteriori* (MAP) estimate of the states given the observed data to construct our spectral estimators as well as statistical confidence intervals. We further present simulation studies as well as application to human EEG data during sleep which reveal significant performance gains achieved by our proposed method.

## II. PROBLEM FORMULATION

Consider a finite realization of  $T$  samples from a discrete-time nonstationary process  $y_t, t = 1, 2, \dots, T$ , obtained via sampling a continuous-time signal above Nyquist rate. We assume that the nonstationary process  $y_t$  is harmonizable so that it admits a Cramér representation [18] of the form:

$$y_t = \int_{-\frac{1}{2}}^{\frac{1}{2}} e^{i2\pi ft} dz(f), \quad (1)$$

where  $dz(f)$  is the generalized Fourier transform of the process. This process has a covariance function of the form:

$$\Gamma(t_1, t_2) := \mathbb{E}[y_{t_1} y_{t_2}^*] = \int_{-\frac{1}{2}}^{\frac{1}{2}} \int_{-\frac{1}{2}}^{\frac{1}{2}} e^{i2\pi(t_1 f_1 - t_2 f_2)} \gamma(f_1, f_2) df_1 df_2, \quad (2)$$

where  $\gamma(f_1, f_2) := \mathbb{E}[dz(f_1) dz^*(f_2)]$  is the generalized spectral density [8]. Due to the difficulty in extracting physically-plausible spectrotemporal information from the two-dimensional function  $\gamma(f_1, f_2)$ , another form of spectrotemporal characterization as a two-dimensional function over time and frequency has gained popularity and is generically referred to as the spectrogram estimate. The spectrogram captures the spectral representation of the data as a function of time, and thus provides a useful framework for analyzing nonstationary time series [19]. A naïve way of estimating such “time-varying” spectral representation is to subdivide the data into overlapping windows or segments and estimate the spectrum for each window independently using various Fourier or wavelet-based methods, under the quasi-stationarity assumption [8]. Though more sophisticated time-varying spectral analysis techniques exist in the literature, such as the Wigner-Ville spectrum [20] and evolutionary spectra [21] and its generalizations [22], the MT based spectrogram is widely-used due to its fast implementation and control over bias-variance trade-off by means of changing the design bandwidth parameters [6]. We refer the reader to [5], [7], [8] for a detailed treatment of the MT method and MT spectrogram estimation.

### A. A State-Space Model for Spectrogram Estimation

Assume, without loss of generality, that an arbitrary window length  $W$  is chosen so that for some integer  $N$ ,  $NW = T$  and let  $\mathbf{y}_n = [y_{(n-1)W+1}, y_{(n-1)W+2}, \dots, y_{nW}]^\top$  for  $n = 1, 2, \dots, N$ , denotes the data within the  $n$ th window. This way, the entire data is divided into  $N$  non-overlapping segments of length  $W$  each. We invoke the quasi-stationarity assumption that  $y_t$  is second-order stationary within each segment of length  $W$ .

Let  $\tilde{y}_t$  be the observation of the signal  $y_t$  corrupted by additive measurement noise, i.e.,  $\tilde{y}_t = y_t + v_t$ , where  $v_t$  is zero mean independent Gaussian noise with variance  $\sigma^2$ . By discretizing the representation in (1) at a frequency spacing of  $2\pi/J$  with  $J$  an integer, at any arbitrary window  $n$ , we have:

$$\tilde{\mathbf{y}}_n = \mathbf{F}_n \mathbf{x}_n + \mathbf{v}_n, \quad (3)$$

where  $\mathbf{F}_n$  is a matrix with elements  $(\mathbf{F}_n)_{l,j} := \exp(i2\pi((n-1)W + l)\frac{j-1}{J})$  for  $l = 1, 2, \dots, W$  and  $j = 1, 2, \dots, J$ ,  $\tilde{\mathbf{y}}_n := [\tilde{y}_{(n-1)W+1}, \tilde{y}_{(n-1)W+2}, \dots, \tilde{y}_{nW}]^\top$  is the noisy observation corresponding to  $\mathbf{y}_n$ ,  $\mathbf{x}_n := [x_n(0), x_n(2\pi\frac{1}{J}), \dots, x_n(2\pi\frac{J-1}{J})]^\top$  denotes a discrete orthogonal increment process, and  $\mathbf{v}_n = [v_{(n-1)W+1}, v_{(n-1)W+2}, \dots, v_{nW}]^\top$  is zero-mean Gaussian noise with covariance  $\text{Cov}\{\mathbf{v}_i, \mathbf{v}_j\} = \sigma^2 \mathbf{I}_{\delta_{i,j}}$ .

Let  $\mathbf{u}^{(k)} := [u_1^{(k)}, u_2^{(k)}, \dots, u_W^{(k)}]^\top$  denote the  $k$ th Slepian sequence or Discrete Prolate Spheroidal Sequence (dpss) used as a taper in the MT method, for  $k = 1, 2, \dots, K$ . Let  $\tilde{\mathbf{y}}_n^{(k)} :=$

$\mathbf{u}^{(k)} \odot \tilde{\mathbf{y}}_n$  be the tapered data at window  $n$  using  $\mathbf{u}^{(k)}$ , where  $\odot$  denotes element-wise multiplication. Finally, let  $x_n^{(k)}(f)$  and  $\mathbf{x}_n^{(k)} := [x_n^{(k)}(0), x_n^{(k)}(2\pi\frac{1}{J}), \dots, x_n^{(k)}(2\pi\frac{J-1}{J})]^\top$  denote the  $k$ th spectral eigen-coefficient of  $\mathbf{y}_n$  and its discretized version respectively, for  $k = 1, 2, \dots, K$ . Then, following (3) we consider the spectrotemporal representation of the tapered data segments as:

$$\tilde{\mathbf{y}}_n^{(k)} = \mathbf{F}_n \mathbf{x}_n^{(k)} + \mathbf{v}_n^{(k)}, \quad (4)$$

where  $\mathbf{v}_n^{(k)}$  is assumed to be independent of  $\mathbf{x}_{1:n-1}^{(k)}$  and identically distributed according to a zero-mean Gaussian distribution with covariance  $\text{Cov}\{\mathbf{v}_i^{(k)}, \mathbf{v}_j^{(k)}\} = \sigma^{(k)2} \mathbf{I}_{\delta_{i,j}}$ . Under this model, we view  $\tilde{\mathbf{y}}_n^{(k)}$  as a noisy observation corresponding to the true eigen-coefficient  $\mathbf{x}_n^{(k)}$ , which provides a linear Gaussian forward model for the observation process.

In order to capture the evolution of the spectrum and hence systematically enforce temporal smoothness, we impose a stochastic continuity constraint on the eigen-coefficients  $(\mathbf{x}_n^{(k)})_{n=1, k=1}^{N, K}$ , using a first-order difference equation:

$$\mathbf{x}_n^{(k)} = \alpha^{(k)} \mathbf{x}_{n-1}^{(k)} + \mathbf{w}_n^{(k)}, \quad (5)$$

where  $0 \leq \alpha^{(k)} < 1$ , and  $\mathbf{w}_n^{(k)}$  is independent of  $\mathbf{x}_{1:n-1}^{(k)}$  and assumed to be distributed according to a zero-mean Gaussian distribution with diagonal covariance  $\text{Cov}\{\mathbf{w}_i^{(k)}, \mathbf{w}_j^{(k)}\} = \mathbf{Q}_i^{(k)} \delta_{i,j}$ . Under this assumption, the discrete-time process,  $(\mathbf{x}_n^{(k)})_{n=1}^N$  forms a jointly Gaussian random process with independent increments, while the process itself is statistically dependent. An estimate of the unobserved states (true eigen-coefficients) from the observations (tapered data) under this model is expected to suppress the measurement noise and capture the true state dynamics.

### B. The Inverse Problem

We formulate the spectral estimation problem as one of Bayesian estimation, in which the Bayesian risk/loss function, fully determined by the posterior density of  $(\mathbf{x}_n^{(k)})_{n=1, k=1}^{N, K}$  given the observations  $(\mathbf{y}_n^{(k)})_{n=1, k=1}^{N, K}$  is minimized. Under the forward model of (4) and the state-space model of (5), the  $k$ th eigen-coefficient can be estimated by solving the following MAP problem:

$$\min_{\mathbf{x}_1^{(k)}, \mathbf{x}_2^{(k)}, \dots, \mathbf{x}_N^{(k)}} \sum_{n=1}^N \left[ \frac{1}{\sigma^2} \left\| \tilde{\mathbf{y}}_n^{(k)} - \mathbf{F}_n \mathbf{x}_n^{(k)} \right\|_2^2 + (\mathbf{x}_n^{(k)} - \alpha \mathbf{x}_{n-1}^{(k)})^H \mathbf{Q}_n^{(k)-1} (\mathbf{x}_n^{(k)} - \alpha \mathbf{x}_{n-1}^{(k)}) \right], \quad (6)$$

for  $k = 1, 2, \dots, K$ . We call the MAP estimation problem in (6) the Dynamic Bayesian Multitaper (DBMT) estimation problem and denote the respective estimate by the DBMT spectrogram estimate.

Equation (6) is a strictly convex function of  $\mathbf{x}_n^{(k)} \in \mathbb{C}^W$  and  $\mathbf{Q}_n^{(k)} \in \mathbb{S}_{++}^W$  for  $n = 1, 2, \dots, N$ , which can be solved using standard optimization techniques. However, these techniques do not scale well with the data length  $N$ . A careful examination of the log-posterior reveals a block tri-diagonal structure

of the Hessian, which can be used to develop an efficient recursive solution that exploits the temporal structure of the problem. However, the parameters of this state-space model also need to be estimated from the data. In the next section, we show how the EM algorithm can be used to estimate both the parameters and states efficiently from (6).

### III. FAST RECURSIVE SOLUTION VIA THE EM ALGORITHM

In order to solve the MAP problem in (6), we need to find the parameters  $\mathbf{Q}_n^{(k)} \in \mathbb{S}_{++}^W$  and  $\alpha^{(k)} \in (0, 1]$  for  $n = 1, 2, \dots, N$  and  $k = 1, 2, \dots, K$ . If the underlying states were known, one could further maximize the log-posterior with respect to the parameters. This observation can be formalized in the EM framework [14], [23]. To avoid notational complexity, we drop the dependence of various variables on the taper index  $k$  in the rest of this subsection.

By treating  $(\mathbf{x}_n)_{n=1}^N$  as the hidden variables and  $\alpha, \mathbf{Q}_n, n = 1, 2, \dots, N$  as the unknown parameters to be estimated, we can write the complete log-likelihood as:

$$\log L(\alpha, \mathbf{Q}_{1:N}) := - \sum_{n=1}^N \left[ \frac{1}{\sigma^2} \|\tilde{\mathbf{y}}_n - \mathbf{F}_n \mathbf{x}_n\|_2^2 + \log |\mathbf{Q}_n| + (\mathbf{x}_n - \alpha \mathbf{x}_{n-1})^H \mathbf{Q}_n^{-1} (\mathbf{x}_n - \alpha \mathbf{x}_{n-1}) \right] + \text{cnst.} \quad (7)$$

For simplicity of exposition, we assume that  $\mathbf{Q}_n = \mathbf{Q}$  for  $n = 1, 2, \dots, N$ . The forthcoming treatment can be extended to the general case with minor modifications. Also, note that  $\sigma^2$  can be absorbed in  $\mathbf{Q}$ , and thus is assumed to be known. An implementation of the EM procedure is described in Algorithm 1. At the  $l^{\text{th}}$  iteration of the EM algorithm, we have:

1) *E-Step*: Given  $\alpha^{[l]}, \mathbf{Q}^{[l]}$ , for  $n = 1, 2, \dots, N$ , the expectations,  $\mathbf{x}_{n|N} := \mathbb{E}[\mathbf{x}_n | \tilde{\mathbf{y}}_{1:N}, \alpha^{[l]}, \mathbf{Q}^{[l]}]$ ,  $\Sigma_{n|N} := \mathbb{E}[(\mathbf{x}_n - \mathbf{x}_{n|N})(\mathbf{x}_n - \mathbf{x}_{n|N})^H | \tilde{\mathbf{y}}_{1:N}, \alpha^{[l]}, \mathbf{Q}^{[l]}]$ ,  $\Sigma_{n,n-1|N} := \mathbb{E}[(\mathbf{x}_n - \mathbf{x}_{n|N})(\mathbf{x}_{n-1} - \mathbf{x}_{n-1|N})^H | \tilde{\mathbf{y}}_{1:N}, \alpha^{[l]}, \mathbf{Q}^{[l]}]$ , can be calculated using the Fixed Interval Smoother (FIS) [24] (lines 4 and 5) and the state-space covariance smoothing algorithm [25] (line 6). These expectations can be used to compute the expectation of the complete data log-likelihood,  $\mathbb{E}[\log L(\alpha, \mathbf{Q}) | \tilde{\mathbf{y}}_{1:N}, \alpha^{[l]}, \mathbf{Q}^{[l]}]$ .

2) *M-Step*: The parameters for the subsequent iteration,  $\alpha^{[l+1]}$  and  $\mathbf{Q}^{[l+1]}$ , can be obtained by maximizing the expectation of (7). Although this expectation is convex in  $\alpha$  and  $\mathbf{Q}$  individually, it is not convex in both. Hence, we perform cyclic iterative updates for  $\alpha^{[l+1]}$  and  $\mathbf{Q}^{[l+1]}$  given in line 8 of Algorithm 1. Once DBMT estimates of all  $K$  eigen-coefficients,  $\hat{\mathbf{x}}_n^{(k)}$  for  $n = 1, 2, \dots, N$  and  $k = 1, 2, \dots, K$  are obtained, the DBMT spectrum estimate is constructed as:

$$\hat{D}_n(f_j) = \frac{1}{K} \sum_{k=1}^K \left| (\hat{\mathbf{x}}_n^{(k)})_j \right|^2, \quad (8)$$

where  $f_j := \frac{2\pi(j-1)}{J}$  for  $j = 1, 2, \dots, J$  and  $n = 1, 2, \dots, N$ .

### IV. APPLICATION TO SYNTHETIC AND REAL DATA

We next examine the performance of DBMT spectrogram estimator on synthetic data, and then demonstrate its utility in spectral analysis of human EEG recordings during sleep.

---

### Algorithm 1 The DBMT Estimate of the $k^{\text{th}}$ Eigen-coefficient

---

- 1: Initialize: observations  $\tilde{\mathbf{y}}_{1:N}^{(k)}$ ; initial guess  $\mathbf{x}_{0|0}$ ; initial guess  $\mathbf{Q}^{[0]}$ ; initial conditions  $\Sigma_{0|0}$ ; tolerance  $\text{tol} \in (0, 10^{-3})$ , Maximum Number of iteration  $L_{\max} \in \mathbb{N}^+$ .
  - 2: **repeat**
  - 3:    $l = 0$ .
  - 4:   Forward filter for  $n = 1, 2, \dots, N$ :
 
$$\begin{aligned} \mathbf{x}_{n|n-1} &= \alpha^{[l]} \mathbf{x}_{n-1|n-1} \\ \Sigma_{n|n-1} &= \alpha^{[l]2} \Sigma_{n-1|n-1} + \mathbf{Q}^{[l]} \\ \mathbf{K}_n &= \Sigma_{n|n-1} \mathbf{F}_n^H (\mathbf{F}_n \Sigma_{n|n-1} \mathbf{F}_n^H + \sigma^2 \mathbf{I})^{-1} \\ \mathbf{x}_{n|n} &= \mathbf{x}_{n|n-1} + \mathbf{K}_n (\tilde{\mathbf{y}}_n - \mathbf{F}_n \mathbf{x}_{n|n-1}) \\ \Sigma_{n|n} &= \Sigma_{n|n-1} - \mathbf{K}_n \mathbf{F}_n \Sigma_{n|n-1} \end{aligned}$$
  - 5:   Backward smoother for  $n = N-1, N-2, \dots, 1$ :
 
$$\begin{aligned} \mathbf{B}_n &= \alpha^{[l]} \Sigma_{n|n} \Sigma_{n+1|n}^{-1} \\ \mathbf{x}_{n|N} &= \mathbf{x}_{n|n} + \mathbf{B}_n (\mathbf{x}_{n+1|N} - \mathbf{x}_{n+1|n}) \\ \Sigma_{n|N} &= \Sigma_{n|n} + \mathbf{B}_n (\Sigma_{n+1|N} - \Sigma_{n+1|n}) \mathbf{B}_n^H \end{aligned}$$
  - 6:   Covariance smoothing for  $n = N-1, N-2, \dots, 1$ :
 
$$\Sigma_{n,n-1|N} = \mathbf{B}_{n-1} \Sigma_{n|N}$$
  - 7:   Let  $\hat{\mathbf{X}}^{[l]} := [\mathbf{x}_{1|N}^H, \mathbf{x}_{2|N}^H, \dots, \mathbf{x}_{N|N}^H]^H$ .
  - 8:   Update  $\alpha^{[l+1]}$  and  $\mathbf{Q}^{[l+1]}$  as:
 
$$\begin{aligned} \alpha^{[l+1]} &= \frac{\sum_{n=2}^N \text{Tr}(\Sigma_{n,n-1|N} \mathbf{Q}^{[l-1]}) + \mathbf{x}_{n-1|N}^H \mathbf{Q}^{[l-1]} \mathbf{x}_{n|N}}{\sum_{n=2}^N \text{Tr}(\Sigma_{n-1|N} \mathbf{Q}^{[l-1]}) + \mathbf{x}_{n-1|N}^H \mathbf{Q}^{[l-1]} \mathbf{x}_{n-1|N}}, \\ \mathbf{Q}^{[l+1]} &= \frac{1}{N} \sum_{n=1}^N [\mathbf{x}_{n|N} \mathbf{x}_{n|N}^H + \Sigma_{n|N} + \alpha^{[l+1]2} (\mathbf{x}_{n-1|N} \mathbf{x}_{n-1|N}^H + \Sigma_{n-1|N}) - \alpha^{[l+1]} (\mathbf{x}_{n-1|N} \mathbf{x}_{n|N}^H + \mathbf{x}_{n|N} \mathbf{x}_{n-1|N}^H + 2\Sigma_{n,n-1|N})]. \end{aligned}$$
  - 9:   Set  $l \leftarrow l + 1$ .
  - 10: **until**  $\frac{\|\hat{\mathbf{X}}^{[l]} - \hat{\mathbf{X}}^{[l-1]}\|_2}{\|\hat{\mathbf{X}}^{[l]}\|_2} < \text{tol}$  or  $l = L_{\max}$ .
  - 11: Output: Denoised eigen-coefficients  $\hat{\mathbf{X}}^{[L]}$  where  $L$  is the index of the last iteration of the algorithm, and error covariance matrices  $\Sigma_{n|N}$  for  $n = 1, 2, \dots, N$  from last iteration of the algorithm.
- 

#### A. Application to Synthetic Data

We synthesize a linear combination of an amplitude-modulated and a frequency-modulated process with high dynamic range for testing the performance of our algorithm. The amplitude-modulated component  $y_t^{(1)}$  is an AR(6) process tuned around 11 Hz, modulated by a cosine at frequency  $f_0 = 0.02$  Hz. The frequency-modulated component  $y_t^{(2)}$  is a realization of an ARMA(6, 4) process with varying pole loci (pair of 3rd order poles at  $\omega_t := 2\pi f_t$  and  $-\omega_t$  with  $f_t$  increasing from 5 Hz, starting at  $t = 0$ , every  $\sim 26$  s by increments of 0.48 Hz). In summary, the noisy observations are given by:

$$y_t = y_t^{(1)} \cos(2\pi f_0 t) + y_t^{(2)} + \sigma v_t, \quad (9)$$

where  $v_t$  is a standard white Gaussian noise process and  $\sigma$  is chosen to achieve an SNR of 30 dB. The process is truncated at 600 s to be used for spectrogram analysis. Figure 1 shows the true as well as estimated spectrograms by the sliding window MT and DBMT estimators. In each row, the left panel shows

the entire spectrogram and the right panel shows the PSD along with confidence intervals (CI) at a selected time point marked by a dashed vertical line in the left panel. For the MT estimate, the CIs are constructed assuming a  $\chi_{2K}^2$  distribution of the estimates around the true values [26], whereas for DBMT estimate by mapping the Gaussian confidence intervals for  $\hat{\mathbf{x}}_n^{(k)}$ 's to the final DBMT estimate.

Figure 1A and B show true spectrogram of the synthetic process and sliding window MT spectrogram estimate respectively. We use windows of length 6 s and the first 3 tapers corresponding to a time-bandwidth product of 3 and 50% overlap to compute the estimate (note that the same window length, tapers and time-bandwidth product are used for the DBMT estimator). Although the MT spectrogram captures the dynamic evolution of both components, it gets blurred by the background noise and picks up spectral artifacts (i.e., vertical lines) due to window overlap and frequency mixing. Fig. 1C demonstrates how the DBMT spectrogram estimate overcomes these deficiencies of the MT spectrogram: the spectrotemporal localization is sharper and smoother across time, artifacts due to overlapping windows are vanished, and frequency mixing is further mitigated. By comparing the right panels of second and third rows, two important observations can be made: *first*, the DBMT estimate captures the true dynamic range of the original noiseless PSD, while the MT estimate fails to do so. *Second*, the CIs in Fig. 1C as compared to 1B are wider when the signal is weak (e.g., near 5 Hz) and tighter when the signal is strong (e.g., near 11 Hz). The latter observation highlights the importance of the model-based confidence intervals in interpreting the denoised estimates of DBMT: while the most likely estimate (i.e., the mean) captures the true dynamic range of the noiseless PSD, the estimator does not preclude cases in which the noise floor of  $-40$  dB is part of the true signal, while showing high confidence in detecting the spectral content of the true signal that abides by the modeled dynamics. In the spirit of easing reproducibility, we have deposited a

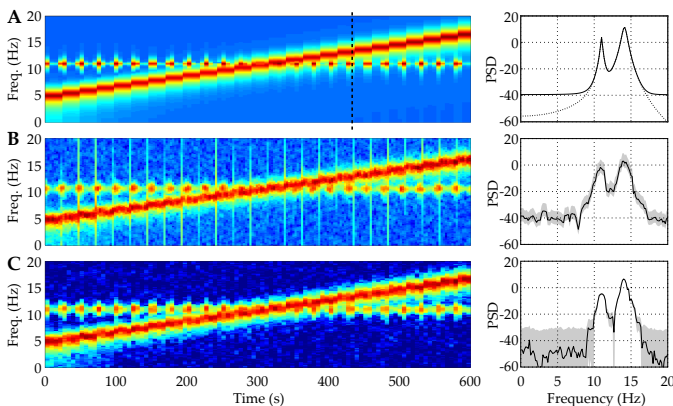


Fig. 1: Spectrogram analysis of the synthetic data. (A) Ground truth, (B) MT estimates, and (C) DBMT estimates. Left: spectrograms. The color scale is in decibels and is calibrated identically for the three subplots. Right: PSDs corresponding to a window of length 6 s starting at  $t = 474$  s. Dashed and solid lines in row A show respectively the noiseless and noisy PSDs. Grey hulls show 95% confidence intervals.

MATLAB implementation of the algorithm 1 on the open source repository GitHub [27], which generates Figure 1.

### B. Application to EEG data

To illustrate the utility of our proposed spectrogram estimator, we apply it to human EEG data during sleep. The data set is available online as part of the SHHS Polysomnography Database (<https://www.physionet.org/pn3/shhpsgdb/>). The EEG data is 900 s long during stage 2 sleep, and sampled at 250 Hz. During stage 2 sleep, the EEG is known to manifest delta waves (0 – 4 Hz) and sleep spindles (transient wave packets with frequency 12 – 14 Hz) [28], [29]. Since the transient spindles occur at a time scale of seconds, we choose a window length of 2.25 s for DBMT algorithm (with 50% overlap for the MT estimate). We also choose a time-bandwidth product of 2.25 for both estimators, in order to keep the frequency resolution at 2 Hz. Figs. 2A and B show the sliding window MT and DBMT spectrogram estimates, respectively, with a similar presentational structure as in Fig. 1. As the right panels reveal, the MT estimate is not able to

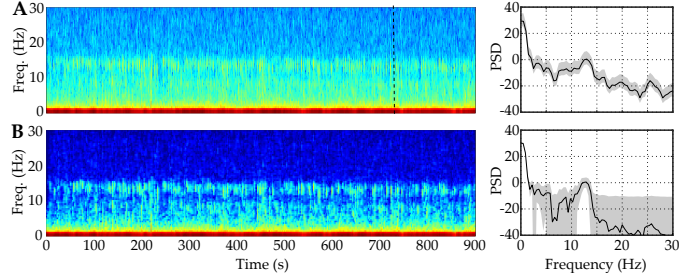


Fig. 2: Spectrogram analysis of the EEG data. (A) MT estimates, and (B) DBMT estimates. Left: spectrograms. The color scale is in decibels and is calibrated identically for the two subplots. Right: PSD estimate corresponding to a window of length 2.25 s starting at  $t = 722.25$  s. Grey hulls show 95% confidence intervals.

clearly distinguish between the delta waves and sleep spindles due to high background noise while the DBMT estimate provides a significantly denoised spectrogram, in which the delta waves and sleep spindles are visually separable. Similar to the analysis of synthetic data, the same observations regarding the CIs of the estimators can be made.

## V. FILTER-BANK INTERPRETATION

By virtue of the FIS procedure under the assumptions that: 1) the window length  $W$  is an integer multiple of  $J$ , the number of discrete frequencies, so that  $\mathbf{F}_n = \mathbf{F}_1, \forall n$ , and 2) the state noise covariance matrices are time-invariant, i.e.,  $\mathbf{Q}_n = \mathbf{Q}, \forall n$ , one obtains the following expansion of  $\mathbf{x}_{n|N}^{(k)}$  in terms of the observed data [17]:

$$\mathbf{x}_{n|N}^{(k)} = \sum_{s=1}^{n-1} \prod_{m=s}^{n-1} [\alpha(\mathbf{I} - \mathbf{K}_m \mathbf{F}_m)] \mathbf{K}_s \mathbf{U}^{(k)} \mathbf{y}_s + \mathbf{K}_n \mathbf{U}^{(k)} \mathbf{y}_n + \sum_{s=n+1}^N \prod_{m=n}^s \mathbf{B}_m \mathbf{K}_s \mathbf{U}^{(k)} \mathbf{y}_s. \quad (10)$$

In other words, the DBMT algorithm maps the entire data  $\mathbf{y} := [y_1, y_2, \dots, y_T]^T$  to the vector of coefficients  $\widehat{\mathbf{X}}^{(k)}$  according to [17]:

$$\widehat{\mathbf{X}}^{(k)} = \mathbf{G}^{(k)} \mathbf{F}^H \mathbf{U}^{(k)} \mathbf{y}, \quad (11)$$

where  $\mathbf{F}$  and  $\mathbf{U}^{(k)}$  are block-diagonal matrices with  $\mathbf{F}_1$  and  $\mathbf{U}_k := \text{diag}[\mathbf{u}^{(k)}]$  as the diagonal blocks, respectively, and  $\mathbf{G}^{(k)}$  is a weighting matrix that depends only on  $\mathbf{Q}_\infty^{(k)} := \lim_{l \rightarrow \infty} (\mathbf{Q}^{(k)})^{[l]}$ ,  $\alpha_\infty^{(k)} := \lim_{l \rightarrow \infty} (\alpha^{(k)})^{[l]}$ , and window length,  $W$ . The rows of  $\mathbf{G}^{(k)} \mathbf{F}^H \mathbf{U}^{(k)}$  form a filter bank whose output is equivalent to the time-frequency representation.

For illustration purpose, the equivalent filters of the DBMT estimator for the 11Hz and 9Hz frequencies around 300 secs from the synthetic data example are shown in Fig. 3. They are also compared to the equivalent filters corresponding to MT method in the frequency domain. As apparent from Fig. 3, the weighting matrix sets the gain of these filters in an adaptive fashion across *all* windows, unlike the standard MT

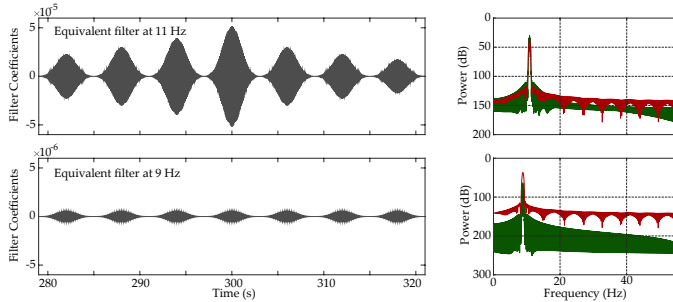


Fig. 3: Equivalent filters corresponding to the DBMT estimate of the synthetic data example. Left: equivalent filters in time around  $t = 300$  s. Right: equivalent filters of DBMT (red) and MT (green) in frequency.

which only uses the data in window  $n$ . In addition, the filter corresponding to frequency of 9Hz, which is negligible in the data, is highly attenuated, resulting in significant noise suppression. In this sense, the proposed estimation method can be viewed as a data-driven denoising method for constructing time-frequency representations given noisy time series data.

## VI. CONCLUDING REMARKS

The classical nonparametric spectral analysis resorts to overlapping windows for capturing temporal smoothness of nonstationary time series data implicitly, ignoring the inherent smoothness of the data. In this paper, we provide an alternative to this paradigm by modeling the temporal dynamics of the spectrum using a state-space model over the eigen-coefficients obtained by multitapering. The proposed algorithm, called DBMT, admits efficient and simple implementation, thanks to the Expectation-Maximization algorithm and the fixed interval state-space smoothing procedure, and operates in a fully data-driven fashion. In the analysis of simulated data and EEG recordings, the DBMT estimates appear to be smoother in time while significantly suppressing the additive noise in comparison to standard MT estimates. In short, the DBMT algorithm is a computationally efficient spectrogram estimator

which inherits the optimality properties of both Bayesian estimators and multitaper analysis.

## REFERENCES

- [1] T. F. Quatieri, *Discrete-time Speech Signal Processing: Principles and Practice*. Prentice Hall, 2008.
- [2] G. Buzsaki, *Rhythms of the Brain*. Oxford University Press, 2009.
- [3] W. J. Emery and R. E. Thomson, *Data analysis methods in physical oceanography*. Elsevier Science, 2001.
- [4] Ö. Yilmaz, *Seismic data analysis: processing, inversion, and interpretation of seismic data*. SEG Books, 2001, no. 10.
- [5] D. J. Thomson, "Spectrum estimation and harmonic analysis," *Proc. IEEE*, vol. 70, no. 9, pp. 1055–1096, Sept 1982.
- [6] T. P. Bronez, "On the performance advantage of multitaper spectral analysis," *IEEE Trans. Signal Process.*, vol. 40, no. 12, pp. 2941–2946, 1992.
- [7] B. Babadi and E. N. Brown, "A review of multitaper spectral analysis," *IEEE Trans. Biomed. Eng.*, vol. 61, no. 5, pp. 1555–1564, May 2014.
- [8] D. J. Thomson, "Multitaper analysis of nonstationary and nonlinear time series data," in *Nonlinear and nonstationary signal processing*. London, UK: Cambridge Univ. Press, 2000, pp. 317–394.
- [9] B. Efron, *The jackknife, the bootstrap and other resampling plans*. SIAM, 1982.
- [10] N. E. Huang, Z. Shen, S. R. Long, M. C. Wu, H. H. Shih, Q. Zheng, N.-C. Yen, C. C. Tung, and H. H. Liu, "The empirical mode decomposition and the Hilbert spectrum for nonlinear and non-stationary time series analysis," *Proc. R. Soc. Lond. A.*, vol. 454, no. 1971, pp. 903–995, 1998.
- [11] I. Daubechies, Y. G. Wang, and H.-t. Wu, "Concft: concentration of frequency and time via a multitapered synchrosqueezed transform," *Phil. Trans. R. Soc. A.*, vol. 374, no. 2065, p. 20150193, 2016.
- [12] J. Xiao and P. Flandrin, "Multitaper time-frequency reassignment for nonstationary spectrum estimation and chirp enhancement," *IEEE Trans. Signal Process.*, vol. 55, no. 6, pp. 2851–2860, 2007.
- [13] L. Fahrmeir and G. Tutz, *Multivariate statistical modelling based on generalized linear models*. Springer Science & Business Media, 2013.
- [14] R. H. Shumway and D. S. Stoffer, "An approach to time series smoothing and forecasting using the EM algorithm," *Science*, vol. 3, no. 4, pp. 653–264, July 1982.
- [15] G. Kitagawa, "Non-Gaussian state-space modeling of nonstationary time series," *J. Amer. Statist. Assoc.*, vol. 82, no. 400, pp. 1032–1041, 1987.
- [16] T. Bohlin, "Analysis of EEG signals with changing spectra using a short-word kalman estimator," *Mathematical Biosciences*, vol. 35, no. 3-4, pp. 221–259, 1977.
- [17] D. Ba, B. Babadi, P. L. Purdon, and E. N. Brown, "Robust spectro-temporal decomposition by iteratively reweighted least squares," *Proc. Natl. Acad. Sci.*, vol. 111, no. 50, pp. E5336–E5345, 2014.
- [18] M. Loève, *Probability Theory*. London: D. Van Nostrand Co., 1963.
- [19] J. Hammond and P. White, "The analysis of non-stationary signals using time-frequency methods," *Journal of Sound and Vibration*, vol. 190, no. 3, pp. 419 – 447, 1996.
- [20] L. Cohen, *Time-Frequency Analysis*. Englewood Cliffs, NJ: Prentice-Hall, 1995.
- [21] M. B. Priestley, "Evolutionary spectra and non-stationary processes," *J. R. Stat. Soc. Ser. B Stat. Methodol.*, pp. 204–237, 1965.
- [22] G. Matz, F. Hlawatsch, and W. Kozek, "Generalized evolutionary spectral analysis and the Weyl spectrum of nonstationary random processes," *IEEE Trans. Signal Process.*, vol. 45, no. 6, pp. 1520–1534, 1997.
- [23] A. P. Dempster, N. M. Laird, and D. B. Rubin, "Maximum likelihood from incomplete data via the EM algorithm," *J. R. Stat. Soc. Ser. B Stat. Methodol.*, pp. 1–38, 1977.
- [24] H. E. Rauch, C. T. Striebel, and T. F., "Maximum likelihood estimates of linear dynamic systems," *AIAA Journal*, vol. 3, pp. 1445–1450, August 1965.
- [25] P. D. Jong and M. J. Mackinnon, "Covariances for smoothed estimates in state space models," *Biometrika*, vol. 75, no. 3, p. 601, 1988.
- [26] D. Percival and A. Walden, *Spectral analysis for physical applications*. Cambridge University Press, 1993.
- [27] *Dynamic Bayesian Multitaper Spectral Estimators*. Available on GitHub Repository: <https://github.com/proloyd/DBMT>, 2017.
- [28] L. D. Gennaro and M. Ferrara, "Sleep spindles: an overview," *Sleep Medicine reviews*, vol. 7, no. 5, pp. 423–440, 2003.
- [29] M. Steriade, D. A. McCormick, and T. J. Sejnowski, "Thalamocortical oscillations in the sleeping and aroused brain," *Science*, vol. 262, no. 5134, pp. 679–685, 1993.